3D PRINTING OF CONDUCTIVE NANOCOMPOSITES FOR LIQUID SENSOR APPLICATION

K. Chizari, M. A. Daoud, A. R. Ravindran and D. Therriault*

Laboratory of Multi-scale Mechanics, Mechanical Engineering Department, Research Center for High Performance Polymer and Composite Systems (CREPEC), École Polytechnique de Montreal, C.P. 6079, succ. Centre-Ville, Montreal, QC H3C 3A7, Canada
Email:daniel.therriault@polymtl.ca

Keywords: Nanocomposite, 3D printing, liquid sensor, carbon nanotubes, polylactic acid (PLA)

ABSTRACT

Conductive nanocomposites (CNCs) are promising candidates as replacement for metals where lighter conductive materials are needed. Applications of CNCs in different fields such as electromagnetic interference (EMI) shielding, sensors, and flexible electrodes have been reported. Liquid sensors (LSs) are a special type of sensor that can detect solvents due to their electrical resistivity variation when they get in contact with some liquids (e.g., organic solvents). One of the most important applications of liquid sensors is for detection of leakage in fuel tanks and pipelines for improving the safety especially when the solvents are hazardous. Here we report the fabrication of CNCs by dispersing carbon nanotubes (CNTs) in polylactic acid (PLA) using ball mill mixing method. The CNCs were dissolved in dichloromethane to form a viscous liquid and were used as conductive inks for 3D printing. Electrically conductive scaffold microstructures were fabricated by solvent-cast 3D printing method featuring controllable structural parameters i.e., the distance between the filaments and number of layers. These scaffold microstructures were used as liquid sensors and the influence of the structural parameters on their liquid sensing behavior were investigated. Our experimental results showed that these conductive printed scaffolds can be used as liquid sensor since their resistivity varies when they are in contact with acetone and their sensitivity varies by changing the structural parameters. The optimum distance between the filaments for the better liquid sensitivity was found between 0.5 mm to 1.5 mm for the range investigated. Increasing the thickness of scaffolds by increasing the number of printed layers led to a decrease in sensitivity of the LSs. These results shows how 3D printing can help us to find the optimum structural parameters for liquid sensors which can be further used for the structures in the form of repeated patterns of filaments such as in textiles.

1 INTRODUCTION

Conductive nanocomposites (CNCs) are generally made from a conductive nanofillers dispersed in a polymer matrix. Due to their unique properties such as light weight and ease of forming, CNCs are advanced materials useful for different applications such as sensors [1, 2], electronics [3-6], electromagnetic interference (EMI) shielding [7, 8], lightning strike protection in airplanes [9, 10], etc. Fabrication of polymer based CNCs using various fillers such as carbon nanotubes (CNTs) [11], carbon nanofibers (CNFs) [12], metallic nanowires [13] and graphene [14] have been reported. Nanofillers such as carbon nanotubes that have high conductivity and high aspect ratio are good candidates for making composites useful for electronic applications since adding low amount of these nanofillers can form conductive percolation paths that turns an insulator material into a conductive material. The main advantages of CNTs compared to metal nanowires are their lower density and higher chemical stability because metal nanowires rapidly oxidize when they enter in contact with oxygen in air. Since the production of CNTs is well developed over the past twenty years, their price is now more affordable which enables novel applications.

The utilisation of CNCs for different types of sensors such as gas sensors [15, 16], strain sensors [17-19] and liquid sensors (LSs) [20, 21] have been reported. The mechanism how these sensors function is usually based on the alteration of the electrical conductivity of CNCs when they enter in contact with certain materials or under mechanical stress/strain [2, 17, 18, 22, 23]. In the case of liquid sensors, the electrical conductivity of CNCs varies when immersed in liquid due to a swelling phenomenon [20, 24]. Swelling of CNCs causes the expansion of the polymer matrix which increases the distance between conductive nanofillers and leads to a lower CNCs effective conductivity.

There are several different methods for forming composites such as injection molding, compression molding, solvent cast and 3D printing (3DP). 3DP method is based on making forms from a digitally designed 3D models [25]. 3DP enables us to fabricate structures with precisely defined structural parameters. Since no mold is needed for the fabrication by 3DP method, changing the structural parameters can be done simply by changing the digitally designed 3D model which makes this method favourable for the investigation of the influence of structural parameters on the sensitivity of liquid sensors. Different types of 3DP (e.g., fused deposition modelling (FDM) [25-27], stereolithography [28, 29], selective laser sintering (SLS) [30], solvent-cast 3DP (SC3DP) [31] and UV assisted 3DP (UV3DP) [32, 33]) have been developed so far.

The sensitivity of CNTs/PLA liquid sensors to different solvents has been previously reported [20, 24, 34, 35]. Here we focus mainly on the influence of structural parameter of printed scaffolds on the sensitivity of LSs. Conductive nanocomposites from CNTs dispersed in polylactic acid (PLA) were fabricated using the ball mill mixing method. Liquid sensors in form of scaffolds with different structural parameters were made by 3DP method and the sensitivity of these liquid sensors was tested using acetone as testing liquid.

2 EXPERIMENTAL

Conductive composites of CNTs/PLA were made by dispersing CNTs in polylactic acid (PLA) via ball mill (SPEX SamplePrep 8000M Mixer/Mill) mixing method [36]. First, 2 g of PLA (PLA-4032D, Natureworks LLC) was dissolved in dichloromethane (DCM) with a weight percentage of 10 wt.%. PLA/DCM solution was poured in the ball mill vial and 0.041g of CNTs (Nanocyl NC7000) was added to this solution in order to make a composite with CNTs concentration of 2 wt.%. Five ball mill balls were added inside the vial and the materials were mixed for 30 min. After the mixing, the material was taken out of ball mill vial and dried at room temperature for 24 h.

The liquid sensors were fabricated in forms of multilayer scaffolds by solvent-cast 3D printing. In this method the composite material is dissolved in a volatile solvent to form a viscous liquid. This viscous liquid solidifies after extrusion from a fine nozzle as the solvent quickly evaporates [31, 34, 37]. CNT/PLA composite was dissolved in DCM with a concentration of 30 wt.% in order to make a printable ink [31]. Fig 1 shows the dispensing robot setup used for fabrication of scaffold. CNT/PLA ink was placed inside a syringe with a nozzle of 200 µm inner diameter. The syringe was placed inside a syringe chamber installed on the dispensing robot head (Fisnar I&J2200-4). The extrusion pressure was controlled by a pressure regulator (HP-7X, EFD) connected to the dispensing robot. The extrusion pressure and the speed of printing nozzle were set at about 370 kPa and 0.3 mm/s, respectively.

The liquid sensitivity of the different conductive scaffolds was tested by measuring their electrical conductivity during immersion/drying cycles. The samples were cut in U shape using a metallic blade. The top parts were attached to electrodes connected to Keithley 6517B resistance meter and the bottom part was immersed in the acetone with an immersion/drying time of 120s/600s and their electrical resistivity was tracked using the resistance meter and Labview software. The relative resistance change was calculated by dividing the difference between the actual resistance and the initial resistance of the U shaped samples. Seven immersion/drying cycles were done on each sample and the values of the relative resistance changes are derived from the last four peaks. The error bars of the relative resistance change data are the standard deviation values of these last four peaks.

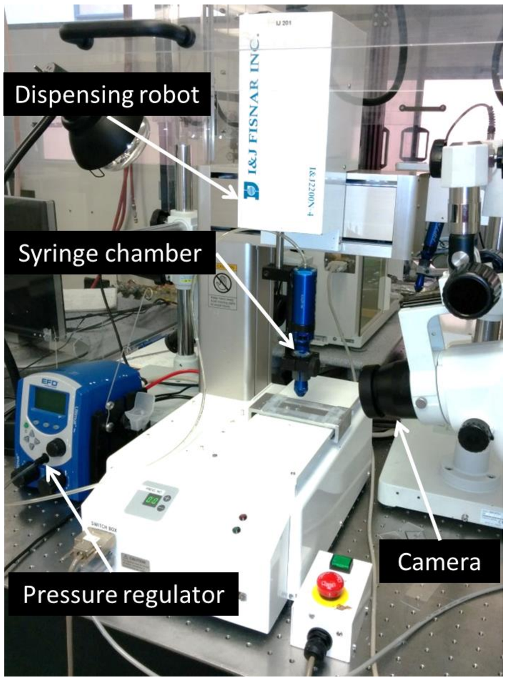

Fig. 1: Fisnar dispensing robot used for 3D printing of scaffold microstructures. A syringe containing CNTs/PLA ink was placed inside the syringe chamber. The 3D printing was done by extrusion of the ink while the nozzle was moving in different directions. The initial position of the nozzle and the extrusion rate were precisely controlled using a camera and a pressure regulator, respectively.

3 RESULTS AND DISCUSSIONS

3.1 3D printing of conductive scaffolds and liquid sensitivity testing

Fig. 2 (a,b) shows SEM images of a scaffold printed using solvent-cast 3D printing method. These scaffolds were cut in U shape (Fig. 2 (c)) before liquid sensing experiments. A typical result of the liquid sensitivity test is shown in Fig. 3.

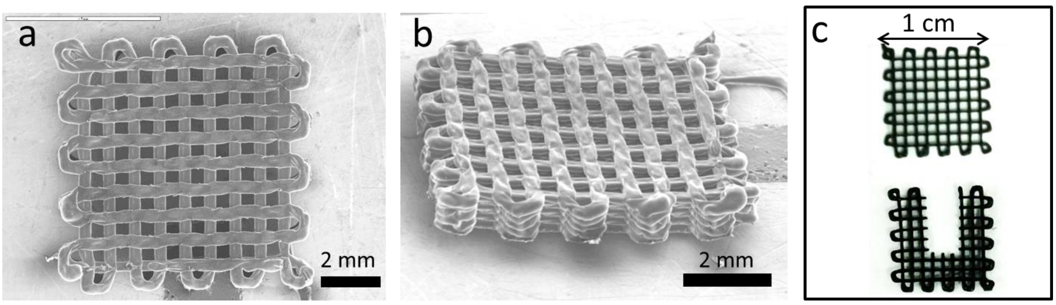

Fig. 2: (a) Top and (b) inclined side view SEM images of a scaffold printed via solvent-cast 3D printing method from a CNTs/PLA composite with 2wt.% of CNTs. The scaffold was printed with a 200 µm nozzle, inter-filament spacing of ~0.7mm and 10 layers (c) Optical photo of CNTs/PLA scaffold and the U- shaped cut sample used for liquid sensing tests (nozzle diameter: 200 µm; space between filaments:~0.7mm; number of layers: 4).

The resistance of the LSs increased when they were immersed in acetone. The increase in the resistivity of LSs can be related to the swelling of PLA matrix which causes an increase of the distance between CNTs nanofillers [21]. Since CNTs are the conductive part of the composite, increasing the distance between the CNTs decreases the number of contacts between them and increases the electrical resistivity of the CNT/PLA composite. The peaks of the relative resistance change at the beginning had lower intensity and by repeating the immersion, their intensity increased until it reached to a plateau value usually after 3 or 4 cycles. Kobashi et al. related the increase in relative resistance change in second immersion to structural variation of CNTs network and PLA matrix due to the solvent left in the structure after the first immersion [21].

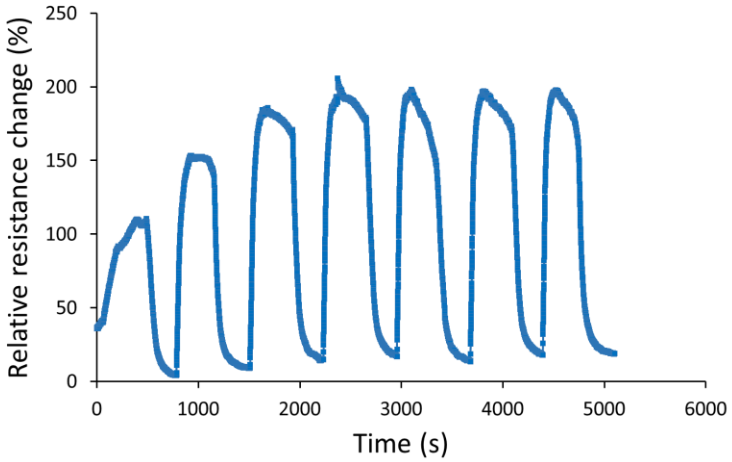

Fig. 3: Relative variation of liquid sensor resistivity when immersed and taken out of acetone. The immersion/drying time was 120/600 s. This scaffold LS was printed with a 200 µm nozzle in four layers with inter-filament spacing of ~0.7 mm.

3.2 Effect of structural parameters on the sensitivity of LSs

The sensitivity behavior of LSs not only depends on the material properties but also to their configuration. The two main structural parameters investigated here are the inter-filament spacing and the number of the layer in the scaffold.

3.2.1 Inter-filament spacing

Various LS scaffolds featuring different inter-filament spacing (IFS) were printed and their liquid sensitivities were tested. A graph showing the influence of IFS on the peak value of the relative resistance change of the LSs is displayed in Fig. 4. The values shown are average values of relative resistance changes of the last four peaks obtained during the liquid sensitivity experiments. The average peak relative resistance varied from ~79% to ~238% when in IFS increased from ~0.21 mm to ~1.0 mm. This value decreased to ~10% by increasing the IFS up to ~ 3.3 mm which can be related to the fact that by increasing the IFS, the scaffolds are not as dense and less material contacts the liquid in the same apparent volume (volume of U shape) which lowers the total electrical conductivity and its variation. The last point of the graph of Fig. 4 belongs to LS printed in form of U without any scaffold structure pattern which was considered as two straight lines configuration for comparison purposes. The U shape without grid like structure had much lower liquid sensitivity. On the other hand if the IFS is too small, the windows that can let the liquid enter the structure are smaller which can hinder the diffusion of the liquid into the structure and lower the total sensitivity of the LS. The optimum IFS found for the printed LSs was in the range of 0.5 to 1.5 mm. The trapping of the solvent in the structure can also influence the sensitivity behavior of the LSs. Guo et al. showed that liquid sensor in helical shape can perform a better liquid sensitivity behavior compared to a single filament since the helical form can trap more liquid due to its unique structure [34]. In the case of scaffolds, increasing the IFS leads to lower amount of liquid trapping which might influence their liquid sensitivity.

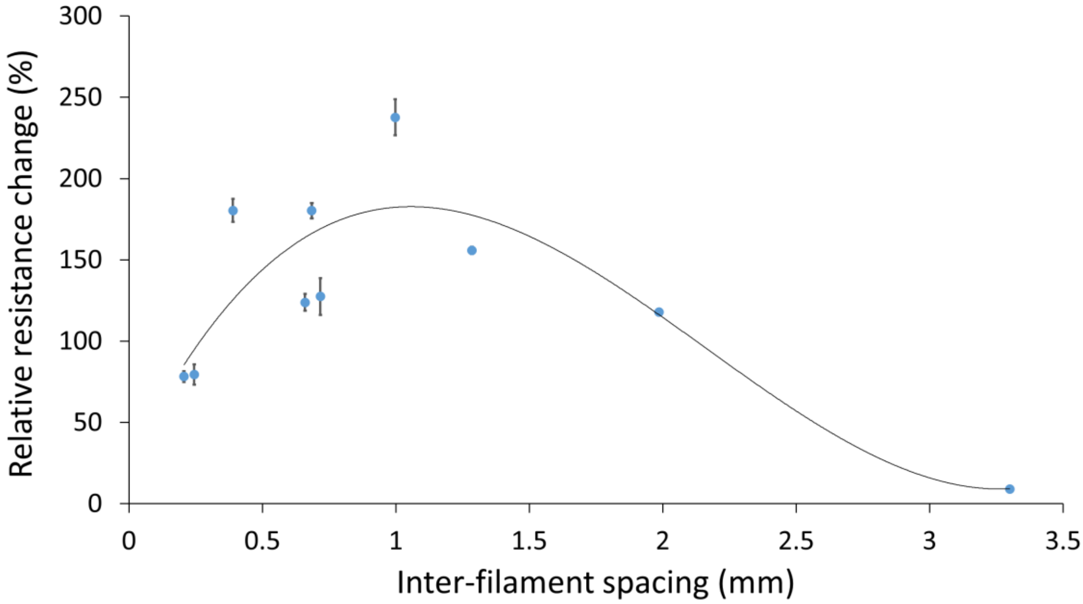

Fig. 4: Graph showing the influence of inter-filament spacing in scaffold structures on the liquid sensitivity of LSs. The highest liquid sensitivity was found for LSs with IFS in the range of 0.5 to 1.5mm with the highest relative resistance change of about 238 % for a scaffold with inter-filament spacing of ~ 1mm. The last point, scaffold with IFS of 3.3 mm, belongs to the sample in a form of an empty U-shape which had the lowest liquid sensitivity.

3.2.2 Scaffold thickness

For a fixed filament diameter, the scaffolds thickness can be controlled by changing the number of printed layers. The influence of the scaffolds thickness on the sensitivity of the LSs was tested for scaffolds with various numbers of layers ranging between 2 to 10 layers. Fig 5 shows the values of peak intensity of relative resistance change as a function of scaffold thicknesses.

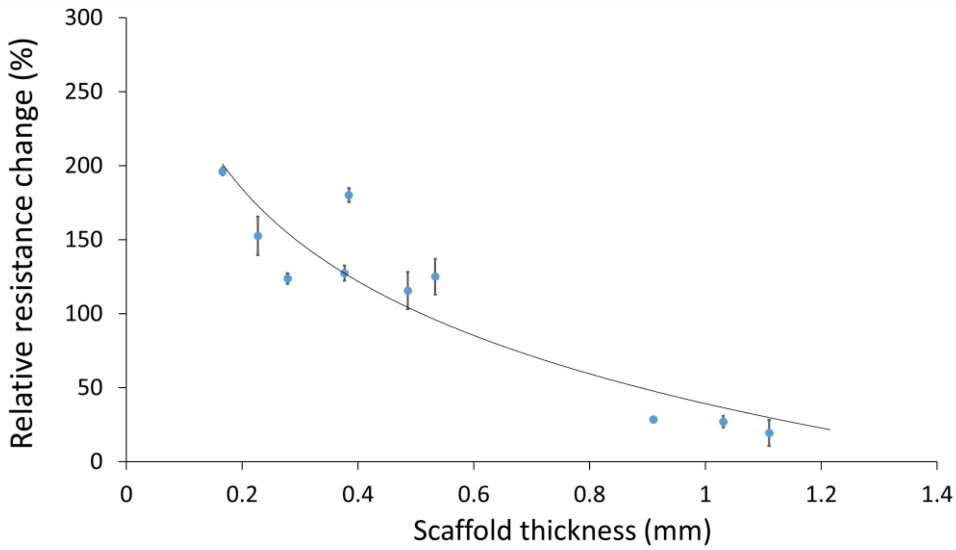

Fig. 5: Relative resistance change of liquid sensors as a function of the scaffold thickness. The thickness of the scaffolds varies from ~0.2mm to ~1.1mm by changing the number of printed layers from 2 to 10. The relative resistance decreased from 196% to 19.5% by increasing the number of layers from 2 to 10.

The highest value of relative resistance change obtained was ~ 196 % for a scaffold made in 2 layers and this value decreased when the number of printed layers increased to 10 layers with a total thickness of about 1.1 mm. The higher liquid sensitivity of thinner LSs can be related to the fact that by decreasing the thickness of the scaffolds the material is more easily exposed to the liquid and so the liquid has less difficulties getting into contact with the surface of the material. Similarly, Kobashi et al. have tested CNT/PLA solid form liquid sensors with thickness in the range of 0.1 to 0.5 mm and reported that the thinner samples resulted in a sharper response and faster recovery of resistance during immersion/drying cycles [20].

4 CONCLUSIONS

Conductive nanocomposites were made from dispersion of CNTs in PLA via ball mill mixing method. CNTs/PLA was dissolved in DCM in order to make a conductive ink compatible with solvent-cast 3D printing. Various scaffolds with different structural parameters were fabricated using this method and their liquid sensing behavior was tested. The results showed that the structural parameters of LSs affect the liquid sensitivity of LSs. The optimum distance between the filaments in scaffold structure is found to be in the range of 0.5 to 1.5 mm. In this condition the liquid can easily enter to the structure and expand the matrix due to swelling phenomenon. Changing the thickness of the scaffolds by varying the number of layers also influenced the liquid sensitivity of LSs in the way that by increasing the printed number of layers from 2 to 10, the overall liquid sensitivity of LSs decreased. This can be related to the difficulties of liquid for diffusion inside the structure and expansion of the PLA matrix in the case of thicker LSs with more compact structures.

One of the most useful forms for liquid sensors is in textile forms which can be wrapped around the area that the leakage needs to be detected [35]. These textiles are consisted of repeated patterns made from woven filaments. In 3D printing method no molding or weaving processes are needed for fabrication of the desired configuration and changing the structural parameters can be done simply by modifying values in the CAD. This work shows the potential of 3D printing method for investigation of the influence of structural parameters in a configuration for a required application such as in liquid sensors. This study will be continued by investigating the influence of other structural parameters such as filament diameter and printed patterns on the liquid sensor behavior of LSs and also the influence of CNTs concentration on their conductivity and liquid sensing.

ACKNOWLEDGEMENTS

The authors acknowledge the financial support from Natural Sciences and Engineering Research Council of Canada (NSERC). We would like to thank Prof. Frédéric Sirois from École Polytechnique de Montréal – Department of Electrical Engineering for providing us technical assistance with the Keithley resistance meter. We also thank Dr. Shuang-Zhuang Guo for his technical assistance with the liquid sensitivity measurements and analyses.

REFERENCES

[1] X. Kang, Z. Mai, X. Zou, P. Cai and J. Mo, A sensitive nonenzymatic glucose sensor in alkaline media with a copper nanocluster/multiwall carbon nanotube-modified glassy carbon electrode. *Analytical Biochemistry*, **363**, 2007, pp. 143-50.

[2] K. Inpil, J.S. Mark, H.K. Jay, S. Vesselin and S. Donglu, A carbon nanotube strain sensor for structural health monitoring. *Smart Materials and Structures*, **15**, 2006, pp. 737.

[3] S. Bae, H. Kim, Y. Lee, X. Xu, J.-S. Park, Y. Zheng, et al., Roll-to-roll production of 30-inch graphene films for transparent electrodes. *Nat Nano*, **5**, 2010, pp. 574-8.

[4] G. Eda and M. Chhowalla, Graphene-based Composite Thin Films for Electronics. *Nano Letters*, **9**, 2009, pp. 814-8.

[5] S. Stankovich, D.A. Dikin, G.H.B. Dommett, K.M. Kohlhaas, E.J. Zimney, E.A. Stach, et al., Graphene-based composite materials. *Nature*, **442**, 2006, pp. 282-6.
[6] J.A. Rogers, T. Someya and Y. Huang, Materials and Mechanics for Stretchable Electronics. *Science*, **327**, 2010, pp. 1603-7.
[7] N. Li, Y. Huang, F. Du, X. He, X. Lin, H. Gao, et al., Electromagnetic interference (EMI) shielding of single-walled carbon nanotube epoxy composites. *Nano Letters*, **6**, 2006, pp. 1141-5.
[8] M. Arjmand, M. Mahmoodi, G.A. Gelves, S. Park and U. Sundararaj, Electrical and electromagnetic interference shielding properties of flow-induced oriented carbon nanotubes in polycarbonate. *Carbon*, **49**, 2011, pp. 3430-40.
[9] M. Gagné and D. Therriault, Lightning strike protection of composites. *Progress in Aerospace Sciences*, **64**, 2014, pp. 1-16.
[10] P.J. Glatkowski, D.H. Landis, J.W. Piche and J.L. Conroy, Carbon nanotube fiber-reinforced composite structures for EM and lightning strike protection. Google Patents 2006.
[11] J. Sandler, M. Shaffer, T. Prasse, W. Bauhofer, K. Schulte and A. Windle, Development of a dispersion process for carbon nanotubes in an epoxy matrix and the resulting electrical properties. *Polymer*, **40**, 1999, pp. 5967-71.
[12] M.H. Al-Saleh and U. Sundararaj, A review of vapor grown carbon nanofiber/polymer conductive composites. *Carbon*, **47**, 2009, pp. 2-22.
[13] S. De, T.M. Higgins, P.E. Lyons, E.M. Doherty, P.N. Nirmalraj, W.J. Blau, et al., Silver nanowire networks as flexible, transparent, conducting films: extremely high DC to optical conductivity ratios. *ACS Nano*, **3**, 2009, pp. 1767-74.
[14] S. Stankovich, D.A. Dikin, G.H. Dommett, K.M. Kohlhaas, E.J. Zimney, E.A. Stach, et al., Graphene-based composite materials. *Nature*, **442**, 2006, pp. 282-6.
[15] K.H. An, S.Y. Jeong, H.R. Hwang and Y.H. Lee, Enhanced Sensitivity of a Gas Sensor Incorporating Single-Walled Carbon Nanotube–Polypyrrole Nanocomposites. *Advanced Materials*, **16**, 2004, pp. 1005-9.
[16] K.G. Ong, K. Zeng and C.A. Grimes, A wireless, passive carbon nanotube-based gas sensor. *Sensors Journal, IEEE*, **2**, 2002, pp. 82-8.
[17] N. Hu, Y. Karube, M. Arai, T. Watanabe, C. Yan, Y. Li, et al., Investigation on sensitivity of a polymer/carbon nanotube composite strain sensor. *Carbon*, **48**, 2010, pp. 680-7.
[18] E.T. Thostenson and T.W. Chou, Carbon Nanotube Networks: Sensing of Distributed Strain and Damage for Life Prediction and Self Healing. *Advanced Materials*, **18**, 2006, pp. 2837-41.
[19] R.D. Farahani, H. Dalir, V. Le Borgne, L.A. Gautier, M.A. El Khakani, M. Lévesque, et al., Direct-write fabrication of freestanding nanocomposite strain sensors. *Nanotechnology*, **23**, 2012, pp. 085502.
[20] K. Kobashi, T. Villmow, T. Andres and P. Pötschke, Liquid sensing of melt-processed poly (lactic acid)/multi-walled carbon nanotube composite films. *Sensors and Actuators B: Chemical*, **134**, 2008, pp. 787-95.
[21] K. Kobashi, T. Villmow, T. Andres, L. Häußler and P. Pötschke, Investigation of liquid sensing mechanism of poly (lactic acid)/multi-walled carbon nanotube composite films. *Smart Materials and Structures*, **18**, 2009, pp. 035008.
[22] T. Yamada, Y. Hayamizu, Y. Yamamoto, Y. Yomogida, A. Izadi-Najafabadi, D.N. Futaba, et al., A stretchable carbon nanotube strain sensor for human-motion detection. *Nat Nano*, **6**, 2011, pp. 296-301.

[23] D.J. Lipomi, M. Vosgueritchian, B.C.K. Tee, S.L. Hellstrom, J.A. Lee, C.H. Fox, et al., Skin-like pressure and strain sensors based on transparent elastic films of carbon nanotubes. *Nat Nano*, **6**, 2011, pp. 788-92.
[24] K. Kazufumi, V. Tobias, A. Timo, H.l. Liane and P. Petra, Investigation of liquid sensing mechanism of poly(lactic acid)/multi-walled carbon nanotube composite films. *Smart Materials and Structures*, **18**, 2009, pp. 035008.
[25] S.S. Crump, inventor Google Patents, assignee. Apparatus and method for creating three-dimensional objects. 1992.
[26] D.W. Hutmacher, Scaffolds in tissue engineering bone and cartilage. *Biomaterials*, **21**, 2000, pp. 2529-43.
[27] D.T. Pham and R.S. Gault, A comparison of rapid prototyping technologies. *International Journal of Machine Tools and Manufacture*, **38**, 1998, pp. 1257-87.
[28] P.F. Jacobs. Stereolithography and other RP&M technologies: from rapid prototyping to rapid tooling: Society of Manufacturing Engineers; 1995.
[29] X. Zhang, X.N. Jiang and C. Sun, Micro-stereolithography of polymeric and ceramic microstructures. *Sensors and Actuators A: Physical*, **77**, 1999, pp. 149-56.
[30] J.J. Beaman and C.R. Deckard, inventors; Google Patents, assignee. Selective laser sintering with assisted powder handling. 1990.
[31] S.Z. Guo, F. Gosselin, N. Guerin, A.M. Lanouette, M.C. Heuzey and D. Therriault, Solvent-Cast Three-Dimensional Printing of Multifunctional Microsystems. *Small*, **9**, 2013, pp. 4118-22.
[32] R. Farahani, L. Lebel and D. Therriault, Processing parameters investigation for the fabrication of self-supported and freeform polymeric microstructures using ultraviolet-assisted three-dimensional printing. *Journal of Micromechanics and Microengineering*, **24**, 2014, pp. 055020.
[33] L.L. Lebel, B. Aissa, M.A.E. Khakani and D. Therriault, Ultraviolet-Assisted Direct-Write Fabrication of Carbon Nanotube/Polymer Nanocomposite Microcoils. *Advanced Materials*, **22**, 2010, pp. 592-6.
[34] S.-z. Guo, X. Yang, M.-C. Heuzey and D. Therriault, 3D printing of a multifunctional nanocomposite helical liquid sensor. *Nanoscale*, **7**, 2015, pp. 6451-6.
[35] T. Villmow, S. Pegel, A. John, R. Rentenberger and P. Pötschke, Liquid sensing: smart polymer/CNT composites. *Materials Today*, **14**, 2011, pp. 340-5.
[36] K. Chizari and D. Therriault. Fabrication of Conductive Microfilaments and Liquid Sensor from CNTs/PLA Nanocomposites. Design, Manufacturing and Applications of Composites Tenth Workshop 2014: Proceedings of the Tenth Joint Canada-Japan Workshop on Composites, August 2014, Vancouver, Canada: DEStech Publications, Inc; p. 214.
[37] R.D. Farahani, K. Chizari and D. Therriault, Three-dimensional printing of freeform helical microstructures: a review. *Nanoscale,* **6**, 2014, pp. 10470-85.